

Robust quantization of a molecular motor motion in a stochastic environment.

V. Y. Chernyak

*Department of Chemistry, Wayne State University,
5101 Cass Avenue, Detroit, MI 48202 and Theoretical Division,
Los Alamos National Laboratory, Los Alamos, NM 87545 USA*

N. A. Sinitsyn

*Center for Nonlinear Studies and Computer, Computational and Statistical Sciences Division,
Los Alamos National Laboratory, Los Alamos, NM 87545 USA*

(Dated: April 18, 2022)

Motivated by experiments with catenane molecules [Leigh *et al Nature (London)* **424** 174 (2003)], we explore quantization of the response of a molecular motor to periodic modulation of control parameters. We formulate a generic exact result, referred to as the Pumping-Quantization Theorem (PQT) that identifies the conditions for robust integer quantized behavior of a periodically driven molecular machine. Implication of PQT on experiments with catenane molecules are discussed.

PACS numbers: 03.65.Vf, 05.10.Gg, 05.40.Ca

Introduction. Molecular motors are molecules capable of performing controlled mechanical motion. An important challenge is to achieve robust control even in strongly fluctuating environment, experienced by any nanoscale system at room temperature. It has been well recognized, however, that noise and fluctuations can serve as a tool rather than an obstacle for molecular machines to achieve their tasks [1]. Gentle adiabatic changes of a few control parameters are sufficient to force molecular machines to perform considerable mechanical movements with high efficiency and control [2].

An ability to rotate its parts is a crucial function of a molecular motor. Molecular systems with this function have been already realized [3, 4, 5]. In the experiment [3] controlled step-wise rotation was implemented using 2- and 3-catenane molecules, that have the topology of interlocked rings (n-catenane is made of n rings). Fig 1 shows a 3-catenane molecule, made of two small (mobile) rings, that perform transitions among 3 regions (stations) on the third, larger, ring. These transitions are caused by thermal fluctuations and, alone, may not lead to directed (clockwise or counterclockwise) motion on average. In experiments, the directed motion was induced by modulating the coupling strengths of mobile rings to stations. This forced the smaller rings to orbit around the center of the larger ring while remaining interlocked with it.

In this Letter, we address an experimental observation [3] that a molecular motor can perform robust quantized operations, e.g. making a full mobile ring rotation per cycle in the control parameter space, even though the ring transitions are stochastic. Quantized response has been also found in several stochastic systems [6, 7]. In the future, more advanced nanomechanical systems will be likely created, and it is important to uncover the basic principles of their operation, e.g., to guide the research on chemical synthesis of nanomechanical structures. Here we make a step towards this goal. To achieve quantized

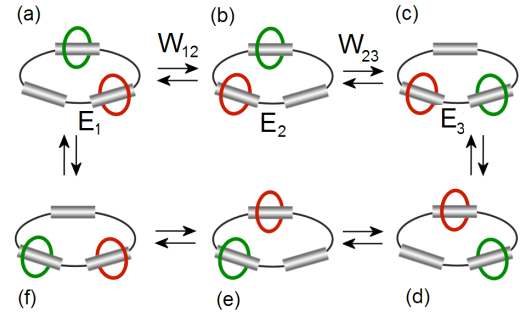


FIG. 1: Topology and metastable states of a 3-catenane molecule.

response in catenane molecules, experiments [3] were performed at sufficiently low temperatures. Therefore, we consider the low temperature limit of a generic stochastic system, and demonstrate that under very general conditions its response to adiabatic periodic parameter modulation should be integer quantized. Next, we show that the integer quantization can be broken and replaced with fractional quantization, if special constraints are imposed on the kinetic rates. We will provide an example, based on the model in Fig. 1, with explicit calculations of the quantized response of a molecule with such a constraint and make prediction for the future experiments.

Integer quantized response of a 3-catenane molecule.

Before considering a general situation, we illustrate the phenomenon of integer quantization using a specific example of a 6-state stochastic model in Fig. 1. The problem of finding the number of rotations can be formulated in terms of stochastic motion on a graph X whose nodes and edges represent the metastable states and allowed transitions, respectively. The transition rates that satisfy the detailed balance can be parameterized by the well depths E_i and potential barriers $W_{ij} = W_{ji}$, so that the kinetic transition rate from the node j to i is given by

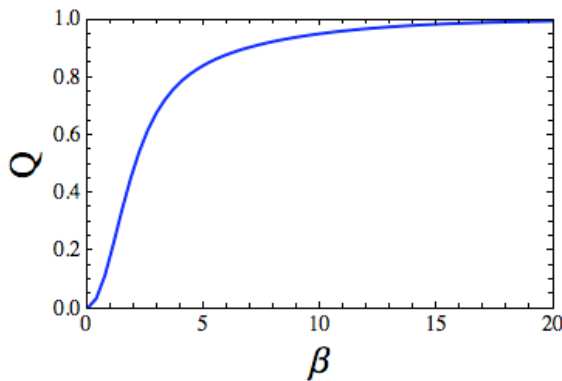


FIG. 2: Average number of rotations of a 3-catenane molecule after adiabatic evolution of control parameters along the contour $\epsilon_1^1 = \cos(\phi)$, $\epsilon_2^2 = \sin(\phi)$, $\phi \in (0, 2\pi)$. Choice of the constant parameters is $\omega_{23}^2 = 1/4$, $\omega_{13}^2 = 1/2$, $\omega_{12}^2 = -1/2$, $\omega_{12}^1 = 0$, $\omega_{23}^1 = -1/8$, $\omega_{13}^1 = -1/7$, $\epsilon_3^1 = 0$, $\epsilon_2^2 = -\epsilon_1^1$, $i = 1, 2, 3$.

$k_{ij} = e^{\beta(E_j - W_{ij})}$, with $\beta = 1/k_B T$ being the inverse temperature. Even if the rates satisfy the detailed balance at any time, periodic changes of the external conditions result in directed particle motion. The phenomenon is referred to as the stochastic pump effect [6, 8].

For the model in Fig. 1, we further express W_{ij} and E_i in terms of the directly controllable parameters, represented by the coupling energies ϵ_j^i of i -th ring to j -th station, or the potential barriers ω_{nm}^i between the station n , occupied by the i -th ring, and an empty station m . By requesting detailed balance to be satisfied and mobile rings be unable to occupy the same station simultaneously, we can relate the energies ϵ_j^i and barriers ω_{nm}^i to E_k and W_{kl} in an effective 6-state model in Fig. 1, e.g. $E_1 = \epsilon_1^1 + \epsilon_2^2$, $E_2 = \epsilon_1^1 + \epsilon_3^3$, $W_{12} = \epsilon_1^1 + \omega_{23}^2$, $W_{23} = \epsilon_3^3 + \omega_{12}^1$, $W_{34} = \epsilon_2^2 + \omega_{13}^1$, etc.

Consider a cyclic adiabatic evolution of ϵ_1^1 and ϵ_2^2 . Fig. 2, shows the dependence of the average number Q of ring rotations per cycle on β , obtained by solving the Master equation in the adiabatic limit. It shows that, generally, the system's response to a periodic parameter variation is not quantized, however, in the low-temperature $\beta \rightarrow \infty$ limit, Q saturates to an integer value $Q = 1$. We have checked for a number of models that the phenomenon is generic. By choosing arbitrary closed contour in the space of control parameters, followed by choosing the other constant parameters randomly, integer response was always achieved in the $\beta \rightarrow \infty$ limit.

The Pumping-Quantization Theorem rationalizes the observation and makes the following assertion: If during the evolution of control parameters no degeneracy of the potential barriers can encounter simultaneously with degeneracy of the minimal well depths, then in the adiabatic and after this low temperature ($\beta \rightarrow \infty$) limits, the average number of particle transitions through any link

of a graph per a driving cycle is an integer. The PQT also *explicitly identifies the quantized current*. We emphasize that by considering $\beta \rightarrow \infty$ limit after the adiabatic approximation we assume that the particle has sufficient time to explore the whole phase space by making stochastic transitions before substantial change of control parameters can happen. Note that in this Letter the word ‘‘theorem’’ in PQT is understood in a physics sense as a general statement, supported by reasonable arguments, referred to as a ‘‘proof’’. A proper statement of an integer PQT, supported by a rigorous proof will be presented in the appendices.

We start with describing the scenario of the stochastic current generation that forms the basis for the proof of the integer PQT. As long as the lowest energy E_j is non-degenerate, the particle sits at site j and no current is generated. When another energy $E_{j'}$ approaches E_j and then becomes smaller, the particle travels from j to j' . Since it is a slow adiabatic process, it is done stochastically, in a variety of ways, generally exploring the whole phase space, avoiding, however, the highest barriers. The latter actually means, as will be demonstrated later using more formal arguments, that complex particle motion during the transition period is restricted to a subgraph $\tilde{X}_{\mathbf{W}} \subset X$ that depends only on the ordering of non-degenerate barriers \mathbf{W} , referred to as the maximal spanning tree. It is constructed from X step-by-step by eliminating the edge with the largest barrier that does not destroy the connectivity. Eventually, when none of the links can be removed without disconnecting the graph, the resulting tree $\tilde{X}_{\mathbf{W}}$ has the following property: the barrier W_{ij} for any withdrawn link $\{i, j\}$ is higher than those of all links of the unique path that connects i to j via $\tilde{X}_{\mathbf{W}}$. Therefore, all paths from j to j' are *homologically equivalent* to the unique shortest path $l_{jj'}(\tilde{X}_{\mathbf{W}})$ that connects j to j' on the tree $\tilde{X}_{\mathbf{W}}$, i.e., they all produce the same current as the one $Q_{jj'}(\tilde{X}_{\mathbf{W}})$, associated with the shortest path. Concatenating the stochastic paths over the consecutive transitions of the protocol period, we obtain a variety of stochastic paths, homologically equivalent to a closed path, represented by the concatenation of $l_{jj'}(\tilde{X}_{\mathbf{W}})$, which *explicitly identifies the generated integer-valued current*.

Our more formal arguments start with the recent observation [8, 9] that, provided the kinetic rates satisfy the detailed balance at all times, the average generated current can be viewed as a response to the evolution of the occupation probability vector \mathbf{p} on the graph nodes, and written as a contour integral along the path \mathbf{s} of the probability vector:

$$Q_{ij}(\mathbf{s}) = \int_{\mathbf{s}} \sum_k A_{ij}^k d\mathbf{p}_k. \quad (1)$$

Here, Q_{ij} is the average number of times the particle passed through the link (i, j) , whereas A_{ij}^k are the components of the vector potential (gauge field) \mathbf{A} , a vector

in the space of currents and a co-vector to the space of probability vectors. Our arguments include three consecutive steps.

(i) We identify \mathbf{A} as the solution of a simple linear problem.

$$(\mathbf{A}^k - \mathbf{A}^{k'}, \mathbf{J})_{\hat{g}} = 0, \quad \sum_j (A_{ij}^k - A_{ij}^{k'}) = \delta_i^k - \delta_i^{k'}, \quad (2)$$

for any conserving $\partial \mathbf{J} = 0$ current. By introducing a scalar product in the vector space of currents

$$(\mathbf{J}, \mathbf{J}')_{\hat{g}} = \sum_{\{i,j\}} g_{ij} J_{ij} J'_{ij}, \quad (3)$$

with $g_{ij} = e^{\beta W_{ij}}$, and summation running over the graph links, Eq. (2) follows from a representation $\sum_k \mathbf{A}^k dp_k = \hat{g}^{-1} \partial^\dagger \boldsymbol{\zeta}$ with $\boldsymbol{\zeta} = e^{\beta \hat{E}} \hat{L}^{-1} d\mathbf{p}$ and $\hat{L} = \partial \hat{g}^{-1} \partial^\dagger e^{\beta \hat{E}}$, where the notation of [8] is used, so that $(\sum_k \mathbf{A}^k dp_k, \mathbf{J})_{\hat{g}} = \partial \mathbf{J} \cdot \boldsymbol{\zeta} = 0$ for a conserved circulating current $\partial \mathbf{J} = 0$. It is straightforward to verify that \mathbf{A} is fully characterized by the two conditions, given by Eq. (2).

(ii) In the case of no barrier degeneracy this important observation allows for an explicit calculation of $\lim_{\beta \rightarrow \infty} \mathbf{A}^k$. This is achieved by the following construction. For a given set of non-degenerate barriers on X , we consider the minimal spanning tree $\tilde{X}_{\mathbf{W}} \subset X$. Substituting the current \mathbf{J} generated by this path combined with the link $\{i, j\}$ into Eq. (2) and noting that, due to the g_{ij} factor in (3), the edge with the largest barrier dominates the scalar product (2) in the $\beta \rightarrow \infty$ limit, we arrive at $\lim_{\beta \rightarrow \infty} (A_{ij}^k - A_{ij}^{k'}) = 0$. This implies that, being fully restricted to the tree $\tilde{X}_{\mathbf{W}}$, the components of \mathbf{A} are represented by an integer-valued current $\lim_{\beta \rightarrow \infty} (\mathbf{A}^k - \mathbf{A}^{k'}) = \mathbf{Q}_{kk'}(\tilde{X}_{\mathbf{W}})$.

(iii) We partition the time period of a driving protocol into a set of small enough segments, so that for each segment we either encounter only the minimal well depth degeneracy or just the potential barrier degeneracy. We refer to them as to 0- and 1-segments, respectively. If necessary, we merge the consecutive segments of the same type, so that the 0- and 1-segments are alternating. In the $\beta \rightarrow \infty$ limit no current is generated on the 0-segments, due to Eq. (1) and since the populations are concentrated in the nodes j with the lowest value of E_j , which implies $d\mathbf{p} = 0$. Since the 1-segments are connected to the 0-segments, the populations $\mathbf{p}_\alpha, \mathbf{p}'_\alpha$ at the boundary of the 1-segment α are concentrated in well-defined nodes k_α, k'_α , determined by the neighboring 0-segments, so that $\mathbf{Q}_\alpha = \mathbf{A} \cdot (\mathbf{p}'_\alpha - \mathbf{p}_\alpha) = \mathbf{Q}_{k_\alpha k'_\alpha}(\tilde{X}_{\mathbf{W}_\alpha})$. The total current $\mathbf{Q}(s) = \sum_\alpha \mathbf{Q}_\alpha$ is generated by the concatenation of the consecutive paths $l_{k_\alpha k'_\alpha}(\tilde{X}_{\mathbf{W}_\alpha})$ that correspond to the 1-segments. This explicitly identifies the generated integer-valued current $\mathbf{Q}(s)$.

Rigid degeneracies and fractional response quantization. According to PQT, non-integer quantization, found

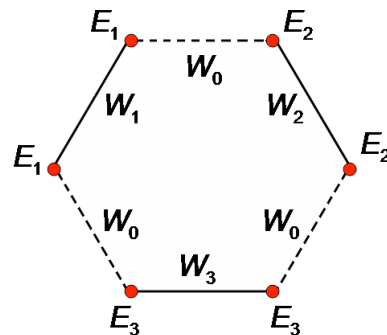


FIG. 3: The 6-state model with degeneracies, including triple degeneracy of barriers and double degeneracy of all well depths.

in experiments with 3-catenane molecules, is highly unlikely when all mobile rings and stations are different and the parameters are in detailed balance. However, in what follows we argue that robust fractional quantization should occur in systems, where, due to some symmetries, permanent (rigid) degeneracy of certain well and/or barriers takes place. To illustrate the point we consider the 3-catenane system in Fig. 1, with a special symmetry: one of the mobile rings, called *active*, has three residence energies ε_j , available for pumping, whereas the other, *passive*, mobile ring has the same constant residing energy $\varepsilon = 0$ for all three stations. All barriers for both rings are constant and identical, equal to ω . The system is described by the Markov-chain model in Fig. 3 defined on the cyclic 6-node graph X with permanently degenerate wells $E_{2j-1} = E_{2j} = \varepsilon_j$, distinct barriers $W_j = \varepsilon_j + \omega$ with $j = 1, 2, 3$, and a permanently degenerate barrier $W_0 = \omega$. The links $\{2j-1, 2j\}$ and $\{2j, 2j+1\}$ describe the transitions when the passive and the active ring, respectively, switches to the non-occupied station.

The considered graph has one cycle, and the currents \mathbf{Q} are single-component. We start with finding the low-temperature limit $\lim_{\beta \rightarrow \infty} \mathbf{A}(\beta)$, hereafter referred to as just \mathbf{A} , in the domain with no degeneracy among the barrier parameters W_j , by using Eq. (2). Let $l_{kk'}^\pm$ be the paths that connect k to k' in the positive and negative directions, respectively, and let $\mathbf{Q}_{kk'}^\pm$ be the corresponding currents generated by the paths. Choosing the conserving $\partial \mathbf{J} = 0$ current in a form $J_{k, k+1} = 1$, we obtain by applying Eq. (2)

$$\mathbf{Q}_{kk'} \equiv \mathbf{A}^{k'} - \mathbf{A}^k = c_{kk'}^+ \mathbf{Q}_{kk'}^+ + c_{kk'}^- \mathbf{Q}_{kk'}^-, \quad (4)$$

with the coefficients $c_{kk'}^\pm$ satisfying the equations

$$c_{kk'}^+ + c_{kk'}^- = 1, \quad c_{kk'}^+ \sum_{\{i,j\} \in l_{kk'}^+} g_{ij} = c_{kk'}^- \sum_{\{i,j\} \in l_{kk'}^-} g_{ij} \quad (5)$$

and in the $\beta \rightarrow \infty$ limit we keep in Eq. (5) only those components g_{ij} that correspond to the maximal barrier W_{ij} . Denoting by $n_{kk'}^\pm(\mathbf{W})$ the number of times

the largest barrier occurs on the links of $l_{kk'}^\pm$, respectively, we obtain from Eq. (5) in the $\beta \rightarrow \infty$ limit $c_{kk'}^\pm(\mathbf{W}) = n_{kk'}^\mp(\mathbf{W})/(n_{kk'}^+(\mathbf{W}) + n_{kk'}^-(\mathbf{W}))$, and combining with Eq. (4) we arrive at

$$\mathbf{Q}_{kk'}(\mathbf{W}) = \frac{n_{kk'}^-(\mathbf{W})\mathbf{Q}_{kk'}^+ + n_{kk'}^+(\mathbf{W})\mathbf{Q}_{kk'}^-}{n_{kk'}^+(\mathbf{W}) + n_{kk'}^-(\mathbf{W})}, \quad (6)$$

which fully describes the vector potential \mathbf{A} with rational components. The total current $\mathbf{Q}(s)$ can be calculated in a way, similar to the integer-quantization case, by partitioning the time period into a set of alternating 0- and 1-segments, with the only difference that the 1-segment generated currents \mathbf{Q}_α are generally rational, since \mathbf{A} and $\mathbf{p}_\alpha, \mathbf{p}'_\alpha$ are rational, the latter are due to equal sharing of the total population between the degenerate lowest-energy wells.

Response quantization and winding index. The protocols under consideration avoid the set Y of “bad” parameters, characterized by simultaneous degeneracy of the lowest wells and highest barriers. A simple analysis of our degenerate model of a 3-catenane molecule shows that Y , as shown in Fig. 4, consists of 4 lines Y_a in the space of $\boldsymbol{\varepsilon} = (\varepsilon_1, \varepsilon_2, \varepsilon_3)$. To understand the global phase diagram of the quantized response, we examine the currents $Q(s)$ generated by small contours $s(\tau) = (\varepsilon + \delta\varepsilon \cos(2\pi\tau), \varepsilon + \delta\varepsilon \sin(2\pi\tau), \varepsilon)$, and $s(\tau) = (-\varepsilon + \delta\varepsilon \cos(2\pi\tau), -\varepsilon, \delta\varepsilon \sin(2\pi\tau))$ around Y_0 and Y_3 . A simple calculation, as described above, which involves 3 and 2 pairs of alternating segments for $a = 0$ and $a = 1, 2, 3$, respectively, yields the currents of 1 and $1/3$, as shown in Fig. 4. The independence of $Q(s)$ on ε and $\delta\varepsilon$ allows the corresponding fluxes $\mathcal{F}_a = 1, 1/3$ to be associated with the lines. It also suggests a topological nature of the quantized current: the response to a general contour is given by the rational winding-index $Q(s) = \sum_a n_a \mathcal{F}_a$, where n_a is the numbers of times the contour encloses the line \mathcal{F}_a , taken with a proper sign depending on orientations (see Fig. 4). Note that the consistency of the winding-index interpretation is provided by the flux conservation at the origin in the parameter space. Similar consideration predicts fractional quantization with a minimal ratio $1/2$ for a system of two identical mobile rings. In the appendices we provide a sample of explicit calculations of a winding number.

Discussion. We have shown that current quantization in a stochastic system is a generic phenomenon and identified the conditions for its observation. PQT directly applies to experiments with catenane molecules predicting integer-quantized response in a generic situation. We showed, however, that additional symmetries can lead to fractional quantization. For example, we predict $1/2$ quantization in a 3-catenane molecule that has two identical rings. We also showed that a 3-catenane molecule can demonstrate fractional quantization with a minimal ratio of $1/3$, which has not been observed previously.

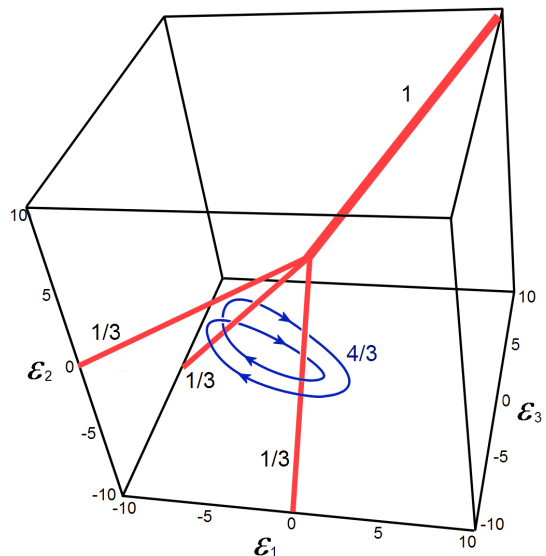


FIG. 4: Topology of the degeneracy space for the active/passive ring model

Quantization of a molecular motor response is topologically protected. This robustness should have applications to the control of nanoscale systems, experiencing thermal fluctuations. Although stochastic transitions can be required for such systems to be operated, the performance can still be controlled with arbitrary precision.

We are grateful to Misha Chertkov and John R. Klein for useful discussions and comments. This material is based upon work supported by NSF under Grant No. CHE-0808910 and in part by DOE under Contract No. DE-AC52-06NA25396.

-
- [1] H. V. Westerhoff et al., *Proc. Natl. Acad. Sci. U.S.A.* **83**, 4734 (1986); P. Hänggi, F. Marchesoni, *Rev. Mod. Phys.* **81**, 387 (2009);
 - [2] D. Astumian, *Proceed. Nat. Acad. Sci. U.S.A.* **104**, 19715 (2007).
 - [3] D. A. Leigh et al., *Nature (London)* **424**, 174 (2003).
 - [4] J. V. Hernandez et al. *Science* **306**, 1532 (2004).
 - [5] J. P. Sauvage, “Molecular machines and motors” *Springer-Verlag Berlin Heidelberg* (2001).
 - [6] For a review, see N. A. Sinitsyn, *J. Phys. A: Theor. Math.* **42**, 193001 (2009).
 - [7] Y. Shi and Q. Niu, *Europhys. Lett.* **59**, 324 (2002).
 - [8] V. Y. Chernyak and N. A. Sinitsyn, *Phys. Rev. Lett.* **101**, 160601 (2008).
 - [9] S. Rahav, J. Horowitz and C. Jarzynski, *Phys. Rev. Lett.* **101**, 140602 (2008).

**INTEGER PUMPING QUANTIZATION
THEOREM (PQT): WEAK VERSION**

In this appendix we formulate a weak version of integer PQT and present a simple proof based on the arguments, presented in the main text. We start with some basic definitions. For our connected non-oriented graph $X = (X_0, X_1; \partial)$, with X_0 , X_1 , and ∂ being the set of nodes, set of links, and boundary map, respectively, let $|X|$ be its geometrical realization (as a CW-complex), $\tilde{\mathcal{M}}_X$ be the space of parameters of our model represented by the sets of the well depths E_j and potential barriers $W_{ij} = W_{ji}$. The subset $\mathcal{M}_X \subset \tilde{\mathcal{M}}_X$ of “good” parameters is defined by the condition that no degeneracy of potential barriers can encounter simultaneously with degeneracy of minimal well depths, i.e., $W_{ij} = W_{kl}$ for some $\{i, j\} \neq \{k, l\}$ implies that if $E_a = E_b$ for some $a \neq b$ then $E_c < E_a$ for some c . We can naturally represent $\mathcal{M}_X = U_0 \cup U_1$ as a union of two open sets, with $U_0 \subset \mathcal{M}_X$ and $U_1 \subset \mathcal{M}_X$ describing the parameters with no minimal well depths and potential barriers degeneracy, respectively. We further denote by $L\mathcal{M}_X$ and $L_\infty\mathcal{M}_X$ the spaces of continuous and smooth maps $S^1 \rightarrow \mathcal{M}_X$, respectively, with $L\mathcal{M}_X$ known as the free loop space of \mathcal{M}_X . A periodic driving protocol $(s, \tau_D) \in L_\infty\tilde{\mathcal{M}}_X \times \mathbb{R}^+$ is represented by its period $\tau_D > 0$ and a smooth free loop $s : S^1 \rightarrow \tilde{\mathcal{M}}_X$. A driving protocol is called “good” if $s \in L_\infty\mathcal{M}_X$. Note that a generic driving protocol is “good”.

Following [8] we denote by $C_0(X; \mathbb{R})$ and $C_1(X; \mathbb{R})$ the vector spaces of populations $\mathbf{p} \in C_0(X; \mathbb{R})$ and currents $\mathbf{J} \in C_1(X; \mathbb{R})$, the latter being described by their components p_i and $J_{kj} = -J_{jk}$, respectively, with $i \in X_0$, $\{k, j\} \in X_1$. We also introduce the chain spaces $C_\bullet(X) \subset C_\bullet(X; \mathbb{R})$ of populations and currents with integer components. The boundary map ∂ , introduced earlier, is obviously extended to the boundary morphism $\partial : C_1(X) \rightarrow C_0(X)$ defined by

$$(\partial\mathbf{J})_i = \sum_j J_{ij}, \quad (7)$$

which is naturally further extended to an operator $\partial : C_1(X; \mathbb{R}) \rightarrow C_0(X; \mathbb{R})$. The subspaces $H_1(X; \mathbb{R}) = \ker\partial$ and $H_1(X) = \ker\partial$ (where ∂ is understood as acting in the spaces of real and integer chains, respectively) are referred to as the spaces of conserving currents. Note that, since $|X|$ is the geometrical realization of a CW-complex we have natural isomorphisms $H_1(X) \cong H_1(|X|)$ and $H_1(X; \mathbb{R}) \cong H_1(|X|; \mathbb{R})$.

The Markov-chain stochastic processes under consideration are described by the master equation, also referred to as the discrete Fokker-Planck (FP), equation

$$d_t\mathbf{p} = \hat{L}(s(t/\tau_D))\mathbf{p} \quad (8)$$

for the evolution in the population space $C_0(X; \mathbb{R})$ that

can be recast using the proper time $\tau = t/\tau_D$ in a form

$$d_\tau\mathbf{p} = \tau_D\hat{L}(s(\tau))\mathbf{p}. \quad (9)$$

As outlined in [8] the FP operator can be represented in a from, convenient for our purposes

$$\hat{L}(s; \beta) = \partial\hat{g}^{-1}\partial^\dagger e^{\beta\hat{E}}, \quad s \in \tilde{\mathcal{M}}_X \quad (10)$$

with $(\hat{E}\mathbf{p})_i = E_i p_i$, and $(\hat{g}\mathbf{J})_{ij} = g_{ij} J_{ij}$, and $\hat{g}(\beta)$ is temperature dependent, according to the definition $g_{ij} = e^{\beta W_{ij}}$, given in the main text. In Eq. (10) $\partial^\dagger : C_0(X; \mathbb{R}) \rightarrow C_1(X; \mathbb{R})$ is the hermitian conjugate with respect to the standard scalar products in the population and current spaces.

The average (with respect to the Markov chain stochastic process) current generated per period defines a map $\mathbf{Q} : L_\infty\tilde{\mathcal{M}}_X \times \mathbb{R}^+ \times \mathbb{R}^+ \rightarrow H_1(|X|; \mathbb{R})$ so that $\mathbf{Q}(\tau_D, \beta) : L_\infty\tilde{\mathcal{M}}_X \rightarrow H_1(|X|; \mathbb{R})$ is the average current per period generated using the driving protocol (s, τ_D) with at the temperature defined by $\beta = 1/(k_B T)$.

It has been outlined by Rahav, Horowitz and Jarzynski [9] that the average current $\mathbf{Q}(s; \tau_D, \beta)$ generated per period can be represented in a form of a contour integral over the driving protocol, given by Eq. (1). Using our notation, this result of [9] can be represented in the following form:

$$\mathbf{Q}(s; \beta, \tau_D) = \int_{\rho(s, \tau_D) \times s} \mathbf{A}, \quad (11)$$

where $\mathbf{A} = \sum_k \mathbf{A}^k dp_k$ is a differential form with coefficients in $C_1(X; \mathbb{R})$ defined on $\tilde{C}_0(X; \mathbb{R}) \times \tilde{\mathcal{M}}_X$, viewed as a smooth manifold, where $\tilde{C}_0(X; \mathbb{R}) \equiv \{\mathbf{p} \in C_0(X; \mathbb{R}) \mid \sum_j p_j = 1 \text{ and } \forall j : 0 < p_j < 1\}$. In Eq. (11) the smooth loop $\rho(s, \tau_D) \in L_\infty\tilde{C}_0(X; \mathbb{R})$ represents the unique periodic solution of Eq. (8) for the driving protocol (s, τ_D) , so that $\rho(s, \tau_D) \times s \in L(\tilde{C}_0(X; \mathbb{R}) \times \tilde{\mathcal{M}}_X)$. We emphasize that Eq. (11) is exact, i.e., it is valid, regardless of whether the driving is adiabatic and temperature is low, or not.

The form \mathbf{A} is fully determined by the following

Proposition .1 *The form in Eq. (11) is fully determined by the following conditions: (i) $\partial\mathbf{A} = \text{id}$, and (ii) $\forall \mathbf{J} \in H_1(X; \mathbb{R}) : (\mathbf{J}, \mathbf{A})_{\hat{g}} = 0$.*

Proof: According to [8, 9], we have

$$\mathbf{A} = \hat{g}^{-1}\partial^\dagger e^{\beta\hat{E}}\hat{L}^{-1}(s, \beta), \quad (12)$$

and applying ∂ to Eq. (12) we reproduce (i) due to the definition of \hat{L} [Eq. (10)]. We further consider a scalar product

$$(\mathbf{J}, \mathbf{A})_{\hat{g}} = (\mathbf{J}, \partial^\dagger e^{\beta\hat{E}}\hat{L}^{-1})_{\hat{g}} = (\partial\mathbf{J}, e^{\beta\hat{E}}\hat{L}^{-1})_{\hat{g}} = 0, \quad (13)$$

which proves statement (ii). ■

Comment: The tangent bundle of $\bar{C}_0(X; \mathbb{R}) \times \tilde{\mathcal{M}}_X$ is trivial with the fiber $\mathbb{T} = \bar{C}_0(X; \mathbb{R}) \oplus \tilde{\mathcal{M}}_X$, where $\bar{C}_0(X; \mathbb{R}) \equiv \{\mathbf{p} \in C_0(X; \mathbb{R}) \mid \sum_j p_j = 0\}$. The differential form \mathbf{A} vanishes on the second component of the tangent space; it represents a connection in a trivial principle bundle over $\bar{C}_0(X; \mathbb{R}) \times \tilde{\mathcal{M}}_X$ with the abelian fiber $C_1(X; \mathbb{R})$. The corresponding holonomy, given by Eq. (11), however, is represented by a conserving current $\partial \mathbf{Q} = 0$ due to Proposition .1, i.e., $\mathbf{Q} \in H_1(X; \mathbb{R})$. This means that \mathbf{A} represents a gauge-equivalence class of connections in a trivial principle bundle over the same base, but with the fiber $H_1(X; \mathbb{R})$, or, equivalently an element of the first differential cohomology.

Formally, integer quantization rests on the fact that, restricted to $\bar{C}_0(X; \mathbb{R}) \times U_1$, the form \mathbf{A} has a well-defined limit $\lim_{\beta \rightarrow \infty} \mathbf{A}(\beta)$. This is established using the minimal spanning tree of a graph X , equipped with linear ordering of its edges. By the definition of $U_1 \subset \tilde{M}_X$, for an element $(\mathbf{E}, \mathbf{W}) \in U_1$ all barriers W_{ij} are non-degenerate and, therefore, provide a linear ordering of the graph edges. The minimal spanning tree is constructed by building a filtration $X = X_0 \supset X_1 \supset \dots \supset X_k \equiv \tilde{X}_{\mathbf{W}}$ applying the following procedure. the subgraph $X_{j+1} \subset X_j$ is obtained from X_j by withdrawing the link with the highest barrier among those, whose elimination keeps the graph connected. The filtration terminates at a tree.

Definition .2 *The tree $\tilde{X}_{\mathbf{W}} \subset X$ that terminates the filtration, constructed above, is called the minimal spanning tree, associated with \mathbf{W} . For any two distinct nodes of X we denote by $l_{ij}(\tilde{X}_{\mathbf{W}})$ the unique path (i_0, \dots, i_r) on $\tilde{X}_{\mathbf{W}}$ with $i_0 = i$ and $i_r = j$ that connects i to j through the maximal spanning tree. We denote by $\mathbf{Q}_{ij}(\tilde{X}_{\mathbf{W}}) \in C_1(X) \subset C_1(X; \mathbb{R})$ the integer current associated with the described path.*

Proposition .3 *The maximal spanning tree $\tilde{X}_{\mathbf{W}}$ has the following property: For any withdrawn edge $\{i, j\}$, i.e., an edge that does not belong to $\tilde{X}_{\mathbf{W}}$ the barrier W_{ij} is higher than any of the barriers associated with the edges of the path $l_{ij}(\tilde{X}_{\mathbf{W}})$.*

Proof: Suppose not, i.e., there is a withdrawn link $\{i, j\}$ so that $W_{i_k i_{k+1}} > W_{ij}$ for some link $\{i_k, i_{k+1}\}$ that belongs to the path $l_{ij}(\tilde{X}_{\mathbf{W}})$. Consider the stage of the filtration building when the link $\{i, j\}$ was withdrawn. By the requirements of the construction withdrawing the link $\{i_k, i_{k+1}\}$ instead of $\{i, j\}$ should turn the graph into a disconnected one, which on the other hand is not true, since the link $\{i_k, i_{k+1}\}$ is a part of a loop, formed by $l_{ij}(\tilde{X}_{\mathbf{W}})$ together with $\{i, j\}$. ■

We are now in a position to describe the low-temperature limit of the form \mathbf{A} .

Proposition .4 *The low-temperature limit $\lim_{\beta \rightarrow \infty} \mathbf{A}$ is well-defined as a locally-constant form, defined over*

$\bar{C}_0(X; \mathbb{R}) \times U_1$. *The convergence is understood in the strong topology sense (uniform convergence) on any subset $C_0(X; \mathbb{R}) \times K$ with compact $K \subset U_1$. The limit is described explicitly by*

$$\lim_{\beta \rightarrow \infty} (\mathbf{A}^k - \mathbf{A}^{k'}) = \mathbf{Q}_{kk'}(\tilde{X}_{\mathbf{W}}). \quad (14)$$

Proof: The proof is based on Proposition .1 that actually claims that \mathbf{A} can be identified by solving a linear problem. We consider the value \mathbf{A} at some point $(\mathbf{p}; \mathbf{E}, \mathbf{W}) \in \bar{C}_0(X; \mathbb{R}) \times U_1$ that, due to Proposition .1 depends on \mathbf{W} only, and evaluate the $\lim_{\beta \rightarrow \infty} \mathbf{A}(\mathbf{W})$. The linear problem that identifies $\mathbf{A}(\mathbf{W})$ can be recast in a form of a linear system that contains a homogeneous equation

$$\mathbf{A}_{ij} + \sum_{\{k, k'\} \in l_{ij}(\tilde{X}_{\mathbf{W}})} g_{ij}^{-1} g_{kk'} \mathbf{A}_{kk'} = 0, \quad (15)$$

with $\{i, j\} \in X_1 \setminus (\tilde{X}_{\mathbf{W}})_1$, and inhomogeneous equation $\partial \mathbf{A} = \text{id}$. Since, by construction of the minimal spanning tree, $g_{ij}^{-1} g_{kk'} \rightarrow 0$ for $\beta \rightarrow \infty$. The linear system has a limit that is of a form

$$\mathbf{A}_{ij} = 0, \quad \forall \{i, j\} \in X_1 \setminus (\tilde{X}_{\mathbf{W}})_1; \quad \partial \mathbf{A} = \text{id}, \quad (16)$$

and $\lim_{\beta \rightarrow \infty} \mathbf{A}(\mathbf{W})$ is a solution of it. We further note that Eq. (16) imply \mathbf{A} to be restricted to $\tilde{X}_{\mathbf{W}}$, where it satisfies the equation $\partial \mathbf{A} = \text{id}$, which obviously has a unique solution. This implies Eq. (14), since $\partial \mathbf{A} = \text{id}$, written in components, reads $(\partial(\mathbf{A}^k - \mathbf{A}^{k'}))_j = \delta_j^k - \delta_j^{k'}$, whereas a straightforward check yields $(\partial \mathbf{Q}_{kk'}(\tilde{X}_{\mathbf{W}}))_j = \delta_j^k - \delta_j^{k'}$.

Uniform convergence on compact subsets is demonstrated in a standard way, the details are not presented here. ■

We are now in a position to formulate and proof a weak version of the integer PQT.

Theorem .5 *For any “good” protocol s there is a well-defined limit $\bar{\mathbf{Q}}(s) \equiv \lim_{\beta \rightarrow \infty} \lim_{\tau_D \rightarrow \infty} \mathbf{Q}(s; \beta, \tau_D)$, so that $\bar{\mathbf{Q}}(s)$ is integer-valued, i.e., $\bar{\mathbf{Q}}(s) \in H_1(|X|) \subset H_1(|X|; \mathbb{R})$.*

Proof: The proof is based on applying the double limit to the integral representation of Eq. (11) with the right hand side evaluated using the properties of the relevant objects, studied above. The $\tau_D \rightarrow \infty$ limit is evaluated in a straightforward way. Since the form \mathbf{A} does not depend on τ_D at all, the limit in Eq. (11) should be applied to just $\boldsymbol{\rho}$. Therefore, $\bar{\mathbf{Q}}(s; \beta) \equiv \lim_{\tau_D \rightarrow \infty} \mathbf{Q}(s; \beta, \tau_D)$ is given by Eq. (11) with $\boldsymbol{\rho}(s, \tau_D)$ replaced with $\boldsymbol{\rho}(s) \equiv \lim_{\tau_D \rightarrow \infty} \boldsymbol{\rho}(s, \tau_D)$. The limit is established by adiabatic theory, which claims $\boldsymbol{\rho}(s)(\tau) = \boldsymbol{\rho}^B(s(\tau))$, with

$$\boldsymbol{\rho}_j^B(\mathbf{E}; \beta) = Z^{-1}(\mathbf{E}; \beta) e^{-\beta E_j}, \quad Z \equiv \sum_j e^{-\beta E_j} \quad (17)$$

being the Boltzmann distribution, so that we have for the generated current in the adiabatic limit

$$\mathbf{Q}(s; \beta) = \int_{S^1} d\tau \mathbf{A}(s(\tau)) d_\tau \boldsymbol{\rho}^B(s(\tau)). \quad (18)$$

To evaluate the $\beta \rightarrow \infty$ limit in Eq. (18) we partition $S^1 = [0, 1]/\{0, 1\}$ into N segments I_α of equal length $\varepsilon = 1/N$. For large enough N we can achieve $s(I_\alpha) \subset U_0$ or $s(I_\alpha) \subset U_1$ for any $\alpha = 1, \dots, N$. This is referred to as I_α being a 0-segment and 1-segment, respectively. If necessary, we merge the consecutive segments of the same type, so that we arrive at a partition $S^1 = \bigcup_\alpha I_\alpha$, where the segments $I_\alpha = [\tau_\alpha, \tau'_\alpha]$ do not necessarily have the same length, however, the type (0- or 1-) of the consecutive segments is alternating. Therefore, the ends $s(\tau_\alpha), s(\tau'_\alpha) \in U_0$ of all $s(I_\alpha)$ belong to U_0 , and we can introduce the nodes k_α and k'_α that correspond to the minimal values of $E_i(\tau_\alpha)$ and $E_i(\tau'_\alpha)$, respectively. Integrating in Eq. (18) over the 1-segments by parts, we obtain for the corresponding contributions

$$\begin{aligned} \mathbf{Q}_\alpha(s; \beta) &= \mathbf{A}(s(\tau'_\alpha)) \tilde{\boldsymbol{\rho}}^B(s(\tau'_\alpha)) - \mathbf{A}(s(\tau_\alpha)) \tilde{\boldsymbol{\rho}}^B(s(\tau_\alpha)) \\ &\quad - \delta \mathbf{Q}_\alpha(s; \beta), \\ \delta \mathbf{Q}_\alpha(s; \beta) &= \int_{I_\alpha} d\tau d_\tau (\mathbf{A}(s(\tau))) \tilde{\boldsymbol{\rho}}^B(s(\tau)), \end{aligned} \quad (19)$$

where $\tilde{\boldsymbol{\rho}}_j^B(\mathbf{E}) \equiv \boldsymbol{\rho}_j^B(\mathbf{E}) - 1/\text{card}(X_0)$ has been introduced to belong to the domain of \mathbf{A} . When applying the $\beta \rightarrow \infty$ limit to Eq. (19) we make use of the fact, that $\lim_{\beta \rightarrow \infty} \rho_j^B(s, \tau_\alpha) = \delta_j^{k_\alpha}$, and that, due to Proposition .4, we have $\lim_{\beta \rightarrow \infty} (\mathbf{A}(s(\tau'_\alpha)) - \mathbf{A}(s(\tau_\alpha))) = 0$. Based on that, we conclude that

$$\lim_{\beta \rightarrow \infty} \mathbf{Q}_\alpha(s; \beta) = \bar{\mathbf{Q}}_\alpha(s) - \lim_{\beta \rightarrow \infty} \delta \mathbf{Q}_\alpha(s; \beta), \quad (20)$$

where

$$\begin{aligned} \bar{\mathbf{Q}}_\alpha(s) &\equiv \lim_{\beta \rightarrow \infty} \mathbf{A}(s(\tau_\alpha)) (\tilde{\boldsymbol{\rho}}^B(s(\tau'_\alpha)) - \tilde{\boldsymbol{\rho}}^B(s(\tau_\alpha))) \\ &= \lim_{\beta \rightarrow \infty} (\mathbf{A}^{k'_\alpha} - \mathbf{A}^{k_\alpha}) = \mathbf{Q}_{k'_\alpha k_\alpha}(\tilde{X}_{\mathbf{W}_\alpha}), \end{aligned} \quad (21)$$

and the last equality is due to Eq. (14).

Therefore, provided

$$\lim_{\beta \rightarrow \infty} \int_{I_\alpha} d\tau \mathbf{A}(s(\tau); \beta) d_\tau \boldsymbol{\rho}^B(s(\tau); \beta) = 0 \quad (22)$$

for all 0-segments, and

$$\lim_{\beta \rightarrow \infty} \int_{I_\alpha} d\tau d_\tau (\mathbf{A}(s(\tau); \beta)) \tilde{\boldsymbol{\rho}}^B(s(\tau); \beta) = 0 \quad (23)$$

for all 1-segments, we arrive at

$$\bar{\mathbf{Q}}(s) = \sum_\alpha \mathbf{Q}_{k'_\alpha k_\alpha}(\tilde{X}_{\mathbf{W}_\alpha}), \quad (24)$$

where the summation runs over all 1-segments, and combined with Definition .2 Eq. (24) yields $\mathbf{Q}(s) \in C_1(X)$. Since, by construction, the 1-segments are alternating with the 0-segments, we have for consecutive 1-segments $k'_\alpha = k_{\alpha+1}$, which implies $\partial \sum_\alpha \mathbf{Q}_{k'_\alpha k_\alpha}(\tilde{X}_{\mathbf{W}_\alpha}) = 0$, or equivalently $\bar{\mathbf{Q}}(s) \in H_1(X)$.

We are not presenting the details on how Eqs. (22) and (23) are derived. This is achieved by making standard estimates. These estimates are based on the fact that $\boldsymbol{\rho}^B(s(\tau); \beta)$ and $\mathbf{A}(s(\tau); \beta)$ are approaching constants exponentially fast when $\beta \rightarrow \infty$ on the 0- and 1-segments, respectively. ■

We conclude this appendix with formulating a stronger version of the weak PQT. A proof will be published elsewhere.

Theorem .6 *There is a weak map $\tilde{Q} : \mathcal{M}_X \rightarrow |X|$ (understood as a morphism in the Quillen's model category associated with the category $\mathcal{T}op$ of topological spaces). Denoting by $\mathbf{Q}_H : H_1(\mathcal{M}_X) \rightarrow H_1(|X|)$ the morphism generated by \tilde{Q} in singular homology, we have a decomposition of the current map $\bar{\mathbf{Q}} : L_\infty \mathcal{M}_X \rightarrow H_1(|X|)$ (defined as a double limit in Theorem .5), described by the following commutative diagram*

$$\begin{array}{ccccc} L_\infty \mathcal{M}_X & \longrightarrow & L\mathcal{M}_X & \longrightarrow & H_1(\mathcal{M}_X) \\ & & & \searrow & \downarrow \mathbf{Q}_H \\ & & & \mathbf{Q} & H_1(|X|) \end{array} \quad (25)$$

where the horizontal morphisms are obvious, and the diagonal maps are compositions.

FRACTIONAL QUANTIZATION: EXAMPLE OF TWO RINGS ON THREE STATIONS WITH PERMANENT DEGENERACY

In this appendix we present some details of the generated current calculations for degenerate models defined on the 6-node cyclic graph X , introduced in the main text (see Fig. 3). We will also comment on the winding-index interpretation of the generated current.

Starting with Eq. (6) we note that the dependence of $n_{kk'}^\pm(\mathbf{W})$ and, therefore, $\mathbf{Q}_{kk'}(\mathbf{W})$ on \mathbf{W} is determined by just the value of $\gamma = 1, 2, 3, 4$ for which W_γ is the highest barrier among the others. Therefore, we will use a convenient and obvious notation $n_{kk',\gamma}^\pm$ and $\mathbf{Q}_{kk',\gamma}$, which allows Eq. (6) to be recast in a form:

$$\mathbf{Q}_{kk',\gamma} = \frac{n_{kk',\gamma}^- \mathbf{Q}_{kk'}^+ + n_{kk',\gamma}^+ \mathbf{Q}_{kk'}^-}{n_{kk',\gamma}^+ + n_{kk',\gamma}^-}, \quad (26)$$

The current generated over a period of a driving protocol can be calculated in a way, similar to the integer-quantization case, by partitioning the time period into a

set of alternating 0- and 1-segments. For a 1-segment let j and j' correspond to lowest energies among E_i on its left and right ends, respectively, and let γ represent the highest barrier on the segment. The current generated over the segment, denoted $\mathcal{Q}_{jj',\gamma}$, can be identified by evaluating the vector potential \mathbf{A} in the $\beta \rightarrow \infty$ limit at the population difference at the ends. Representing the difference of the end populations $p_i = 1/2(\delta_{i,2j-1} + \delta_{i,2j})$ and $p'_i = 1/2(\delta_{i,2j'-1} + \delta_{i,2j'})$, respectively, in a form

$$p'_i - p_i = (\delta_{i,2j'-1} - \delta_{i,2j-1})/2 + (\delta_{i,2j'} - \delta_{i,2j})/2 \quad (27)$$

to be able to use Eqs. (5) and (26) directly, we arrive at

$$\mathcal{Q}_{jj',\gamma} = (\mathcal{Q}_{2j-1,2j'-1;\gamma} + \mathcal{Q}_{2j,2j';\gamma})/2. \quad (28)$$

In the rest of this appendix we provide a simple and intuitive picture of the generated current as a winding index with rational coefficients. The space $Y \subset \tilde{Y}$ of “bad” parameters is included in $\tilde{Y} \equiv \tilde{\mathcal{M}}_X \setminus \mathcal{M}_X$, the latter characterized by simultaneous degeneracy among E_j and W_γ . For an element of \tilde{Y} with $E_j = E_{j'} < E_i, \forall i \neq j, j'$ and $W_\gamma = W_{\gamma'} \neq W_\mu, \forall \mu \neq \gamma, \gamma'$ consider a small loop s that winds around \tilde{Y} in a small neighborhood of the element of the parameter space, introduced above. Such a loop can be represented by a small circle that winds around the $(0,0)$ point in the space of $(E_{j'} - E_j, W_{\gamma'} - W_\gamma)$. The current $\mathcal{Q}(s)$ generated over the period can be easily computed, using the methodology developed above, specifically by partitioning S^1 into alternating two 0- and two 1-segments. The current is generated on the two 1-segments with $W_\gamma < W_{\gamma'}$ and $W_\gamma > W_{\gamma'}$. Note that on the two 0-segments the lowest energies are E_j and $E_{j'}$, respectively. It is easy to see that if $W_\gamma \approx W_{\gamma'}$ is not the highest barrier the currents generated over the two 1-segments cancel each other. Therefore, to achieve a non-zero current we should start with a point with a stronger set of restrictions $W_\gamma = W_{\gamma'} > W_\mu, \forall \mu \neq \gamma, \gamma'$ on the barriers. In this case we calculate

$$\bar{\mathcal{Q}}(s) = \mathcal{Q}_{jj',\gamma} + \mathcal{Q}_{j'j,\gamma'}, \quad (29)$$

to see that the generated current is robust to small perturbations of the loop s . Therefore, we can introduce the subsets $Y_{jj',\gamma\gamma'} \equiv \{(\mathbf{E}, \mathbf{W}) | E_j = E_{j'} < E_i, \forall i \neq j, j' \text{ and } W_\gamma = W_{\gamma'} > W_\mu, \forall \mu \neq \gamma, \gamma'\}$ of the parameter space, and associate with each of them a current “flux” $\mathbf{F}_{jj',\gamma\gamma'} = \mathcal{Q}(s)$ for a properly defined loop s , so that we have

$$\mathbf{F}_{jj',\gamma\gamma'} = \mathcal{Q}_{jj',\gamma} + \mathcal{Q}_{j'j,\gamma'}, \quad (30)$$

and applying Eq. (28) makes the definition of the current “flux” explicit. Note that $\partial \mathbf{F}_{jj',\gamma\gamma'} = 0$, i.e., any current “flux” represents a conserving current, which in the considered example is given by a single rational number. Note that in dealing with “fluxes” orientations are important. The definition of Eq. (29) corresponds to an

orientation, where the 0- and 1-segments alternate in the order (j, γ, j', γ') so that at the 1-segments, labeled by γ and γ' the current flows from j to j' and from j' to j , respectively. Also note that the flux $\mathbf{F}_{jj',\gamma\gamma'}$ is anti-symmetric with respect to the permutations of (j, j') and (γ, γ') .

We further define the subset of “bad” parameters by $Y = \bigcup \bar{Y}_{jj',\gamma\gamma'}$ with $\bar{Y}_{jj',\gamma\gamma'}$ denoting the closure of $Y_{jj',\gamma\gamma'}$. The space Y , equipped with the set $\mathbf{F}_{jj',\gamma\gamma'}$, is referred to as the rational cycle of our model. For any “good” driving protocol the generated current $\bar{\mathcal{Q}}(s)$ can be computed as a winding index: (i) We span a surface \mathcal{A} on s so that $\mathcal{A} \cap Y$ avoids the boundaries of the cells $\bar{Y}_{jj',\gamma\gamma'}$ and the intersections are transversal, (ii) $\bar{\mathcal{Q}}(s)$ is given by the sum of the current “fluxes” \mathbf{F} at the intersection points, accounted with proper signs.

Now we are in position to compute the fluxes for our model explicitly. In our model there are 18 cells $Y_{jj',\gamma\gamma'}$ that correspond to 3 and 6 choices of a degenerated pair of energies and barriers, respectively. By the cyclic symmetry of our model it is enough to find 6 fluxes $F_{12,\gamma\gamma'}$, the other 12 are restored by cyclic permutations. When computing $F_{12,\gamma\gamma'}$ we can also apply a mirror symmetry in permuting $1 \leftrightarrow 2$. Therefore only 4 computations are actually required. In computing the flux, represented by a conserving current, one can monitor the flow through any link on our cyclic graph, since for a conserving current they are all the same. To simplify a calculation we can always choose a link that corresponds to one of non-degenerate (in the sense of permanent degeneracy) degenerate barriers.

A simple calculation shows $F_{12,12} = 0$, $F_{12,13} = F_{12,10} = 1$, and $F_{12,03} = 1/3$. by the mirror symmetry we have $F_{12,32} = F_{12,02} = 1$.

Finally, we build a winding-index interpretation of our original model of two rings jumping between three stations in terms of a more general model, defined on a 6-node cyclic graph X , described above in some detail. This constitutes an example of a general pull-back construction. The parameter space $\tilde{M} \cong \mathbb{R}^3$ of the original model describes the parameter sets $\boldsymbol{\varepsilon} = (\varepsilon_1, \varepsilon_2, \varepsilon_3)$, and its relation to a more general model on the graph X is expressed by the map $p : \tilde{M} \rightarrow \tilde{\mathcal{M}}_X$ that has a form $p(\boldsymbol{\varepsilon}) = (\mathbf{E}, \mathbf{W})$. The space $Y(\tilde{M}) \subset \tilde{M}$ of “bad” parameters is obviously defined as $Y(\tilde{M}) \equiv p^{-1}(Y)$. A simple analysis shows $Y(\tilde{M}) = \bigcup_{a=1}^4 \bar{Y}_a(\tilde{M})$ with $Y_0(M) = \{\boldsymbol{\varepsilon} | \varepsilon_1 = \varepsilon_2 = \varepsilon_3 > 0\}$, $Y_1(M) = \{\boldsymbol{\varepsilon} | \varepsilon_1 = 0, \varepsilon_2 = \varepsilon_3 < 0\}$, and $Y_a(M)$ for $a = 2, 3$ obtained by a cyclic permutation. The corresponding fluxes are denoted $\mathcal{F}_a \in \mathbb{Q}$. The one-point compactification $Y(M)^c \subset S^3 \cong (\mathbb{R}^3)^c$ is a CW-complex of dimension 1 (non-oriented graph) with two nodes $0, \infty \in S^3$, connected by 4 links. For a “good” driving protocol $s : S^1 \rightarrow \tilde{M} \setminus Y(M)$ we can express the generated current $\bar{\mathcal{Q}}(s) = [\mathcal{F}] \star [s]$ as a rational winding index of \mathcal{F} with s .

Since $p(Y_3(\tilde{M})) \subset Y_{12,03}$ for $a = 1, 2, 3$ we have

$\mathcal{F}_3 = \mathcal{F}_{12,03} = 1/3$. Similarly (or by symmetry), $\mathcal{F}_1 = \mathcal{F}_2 = 1/3$. By the flux conservation we obtain $\mathcal{F}_0 = -1$. Note that we have used the orientations of all four fluxes towards the $(0,0,0)$ point. Direct computation of \mathcal{F}_0 is a bit more involved since $p(\mathcal{F}_0)$ belongs to the cell boundaries in $Y \subset \tilde{\mathcal{M}}_X$. It can be still performed in a standard way. For $\varepsilon > 0$ we consider a point $(\varepsilon, \varepsilon, \varepsilon) \in Y_0(M)$ and a loop $s(\tau) = p(\varepsilon(\tau))$ with $\varepsilon(\tau) = (\varepsilon + \delta\varepsilon \cos(2\pi\tau), \varepsilon + \delta\varepsilon \sin(2\pi\tau), \varepsilon)$. The lowest energies are E_3 for $0 < \tau < 1/4$, E_1 for $1/4 < \tau < 5/8$, and E_2 for $5/8 < \tau < 1$. The 1-segments can be chosen to be segments of small enough length, centered around $\tau = 0$, $\tau = 1/4$, and $\tau = 5/8$ with the highest barriers being W_1 , W_2 , and W_3 , respectively. Therefore, the generated current consists of three contributions, related to three 1-segments:

$$\begin{aligned} \mathcal{F}_0 = \bar{\mathcal{Q}}(s) &= (\mathcal{Q}_{35}^+ + \mathcal{Q}_{46}^+)/2 + (\mathcal{Q}_{51}^+ + \mathcal{Q}_{62}^+)/2 \\ &+ (\mathcal{Q}_{13}^+ + \mathcal{Q}_{24}^+)/2, \end{aligned} \quad (31)$$

and a simple calculation shows $\mathcal{F}_0 = -1$.

The fluxes \mathcal{F}_a for $a = 1, 2, 3$, which are equal due to the symmetry, can also be computed directly. Consider, e.g., the flux \mathcal{F}_3 ; it can be calculated using the loop $\varepsilon(\tau) = (-\varepsilon + \delta\varepsilon \cos(2\pi\tau), -\varepsilon, \delta\varepsilon \sin(2\pi\tau))$ that winds around Y_3 . The lowest well is degenerate for $\tau = 1/4$ and $\tau = 3/4$, in both cases it corresponds to $E_1 = E_2$, with the highest barrier being W_3 and W_0 , respectively. The 1-segments can be chosen to be segments of small enough length, centered around $\tau = 1/4$ and $\tau = 3/4$, respectively. Since the generated current $\bar{\mathcal{Q}}(s)$ is conserving, we can monitor any of its component, so we can choose $\bar{\mathcal{Q}}_{56}(s)$ that corresponds to the barrier W_3 . On the 1-segment around $\tau = 1/4$ the highest barrier is W_3 , therefore, no current passes through the chosen link. On the 1-segment around $\tau = 3/4$ the highest barrier W_0 is degenerate, the current that flows through the chosen link $\{5, 6\}$ passes through two highest barriers, whereas the current in the opposite direction passes one highest barrier. Therefore, the latter is twice larger, which means that, according to Eq. (6), the described currents are equal to $1/3$ and $2/3$, respectively. This results in $\mathcal{F}_3 = 1/3$.

The reason why Y , equipped with the set $\mathbf{F}_{jj'\gamma\gamma'}$, is referred to as the rational cycle is as follows. Upon the one-point compactification of $\tilde{\mathcal{M}}_X$, denoted by $\tilde{\mathcal{M}}_X^c$, Y turns into Y^c , the latter having an obvious structure of a CW-complex with $\tilde{Y}_{jj',\gamma\gamma'}^c$ representing the cells of the highest dimension. Therefore, the set $\mathbf{F}_{jj'\gamma\gamma'}$ determines a homology class $[\mathbf{F}] \in H_\bullet(Y^c; \mathbb{Q})$ in the highest dimension. Considering $[s] \in H_1(\tilde{\mathcal{M}}_X^c \setminus Y^c)$ as the homology class generated by the loop s , the generated current $\bar{\mathcal{Q}}(s)$ is given by the winding index $[\mathbf{F}] \star [s] \in \mathbb{Q}$ of $[\mathbf{F}]$ with $[s]$. The last statement is a direct consequence of Poincaré duality in $\tilde{\mathcal{M}}_X^c$ and \tilde{M}^c , combined with its functorial nature. Note that the current-generating rational cycle $\mathcal{F} \in H_{\dim \tilde{M}-2}(Y(\tilde{M})^c; \mathbb{Q})$ of the original

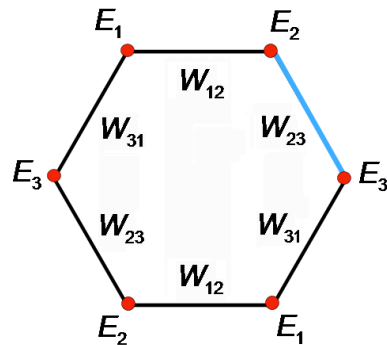


FIG. 5: Parameters representing kinetic rates of the 6-model of catenane molecule with identical mobile rings.

model is pulled back from the corresponding cycle $\mathbf{F} \in H_{\dim \tilde{\mathcal{M}}_X-2}(Y^c; \mathbb{Q})$, i.e., $\mathcal{F} = p_! \mathbf{F}$ by means of the morphism $p_! : H_\bullet(Y^c; \mathbb{Q}) \rightarrow H_{\bullet-\dim \tilde{\mathcal{M}}_X+\dim \tilde{M}}(Y(\tilde{M})^c; \mathbb{Q})$, often referred to as a wrong way map, whose existence can be interpreted as a consequence of Poincaré duality in the spaces $\tilde{\mathcal{M}}_X^c$ and \tilde{M}^c .

EXAMPLE WITH IDENTICAL MOBILE RINGS

In this appendix we study a system of two identical mobile rings jumping among three stations. The system represents the simplest example of random walk of a number of identical particles on a graph under the exclusion constraint that does not allow any site to be occupied by more than one particle. Let the control parameters be represented by the coupling energies ε_i , $i = 1, 2, 3$ of the mobile rings to the i -th stations, whereas all individual barriers are identical and constant, equal to ω . The system is described by the Markov chain model in Fig. 5, defined on a cyclic 6-node graph X . The symmetry that originates from the identical nature of the mobile rings shows itself as an inversion symmetry on the graph X , i.e., the wells and the barriers that correspond to the opposite nodes and links, respectively, are identical. This results in a double degeneracy of all energies and barriers of the 6-state model on the graph X , whose relation to the parameters of the original system is given by

$$\begin{aligned} E_1 &= \varepsilon_1 + \varepsilon_2, \quad E_2 = \varepsilon_1 + \varepsilon_3, \quad E_3 = \varepsilon_2 + \varepsilon_3, \\ W_{12} &= \varepsilon_1 + \omega, \quad W_{23} = \varepsilon_3 + \omega, \quad W_{31} = \varepsilon_2 + \omega. \end{aligned} \quad (32)$$

The set of “bad” parameters Y of the model on the graph X is represented by 9 cells $Y_{jj',\gamma\gamma'}$, which corresponds to 3 and 3 choices of a degenerate pair of energies and barriers. A simple calculation shows that the fluxes that correspond to $Y_{12,23}$, $Y_{23,13}$, and $Y_{31,12}$, which implies that the set of “bad” parameters of the original model is given by $Y_0 = \{(\varepsilon_1, \varepsilon_2, \varepsilon_3) | \varepsilon_1 = \varepsilon_2 = \varepsilon_3\}$. To compute the corresponding flux \mathcal{F}_0 we consider a loop $\varepsilon(\tau) = (\varepsilon + \delta\varepsilon \cos(2\pi\tau), \varepsilon + \delta\varepsilon \sin(2\pi\tau), \varepsilon)$. The lowest

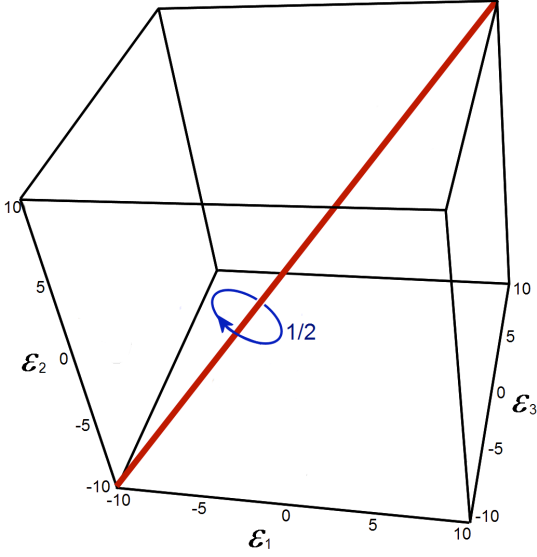


FIG. 6: Topology of the degeneracy space corresponding to 3-catenane molecule with identical mobile rings.

energies are E_3 for $0 < \tau < 1/4$, E_1 for $1/4 < \tau < 5/8$, and E_2 for $5/8 < \tau < 1$. The 1-segments can be chosen to be segments of small enough length, centered around $\tau = 0$, $\tau = 1/4$, and $\tau = 5/8$. At this point we should emphasize that the degeneracy $E_3 = E_1$, $E_1 = E_2$, and

$E_2 = E_3$ of the lowest energies at $\tau = 1/4$, $\tau = 5/8$, and $\tau = 1$, respectively, is accompanied by simultaneous degeneracy $W_{12} = W_{23}$, $W_{23} = W_{31}$, and $W_{12} = W_{31}$ of the highest barriers. However, this does not cause a problem, since, as stated above, the corresponding fluxes $F_{12,23} = F_{23,13} = F_{31,12} = 0$ vanish. This means that any of the degenerate highest barriers can be announced the highest, i.e., we can consider W_{12} , W_{23} , and W_{31} , respectively, to be the highest barriers. Any other allowed choice will lead to the same results due to the vanished corresponding fluxes.

To determine the total current generated per cycle, it is sufficient to find the total current per cycle through any link. Consider, for example the link between states with the energies E_2 and E_3 (marked by blue color in Fig. 5). The transition currents generated at the 1-segments around $\tau = 1/4$ and $\tau = 5/8$ do not contribute to the component associated with the chosen link, since all pathways that avoid the maximal barrier miss the chosen link. The transition current around $\tau = 1$ is equally split between the two pathways represented by the chosen link and opposite to it. This leads to the current of $1/2$ through the chosen link, which results in a rational flux $\mathcal{F}_0 = 1/2$. The flux phase diagram in the space of the control parameters is shown in Fig. 6.